Control of a Class of Underactuated Systems by Successive Submanifold Stabilization ⋆

Fabian Beck * **Noboru Sakamoto** ** **Christian Ott** *

* *Institute of Robotics and Mechatronics, German Aerospace Center (DLR), 82234 Wessling, Germany (e-mail: {firstname}.{lastname}@dlr.de).*
** *Department of Mechanical Engineering and System Control, Nanzan University, Yamzato-cho 18, Showa-ku, Nagoya, 466-8673, Japan (e-mail: noboru.sakamoto@nanzan-u.ac.jp)*

Abstract: Many control design methods for underactuated systems require solving a partial differential equation, which can be complex for systems with many degrees of freedom. In order to reduce the complexity, it is proposed to decompose the dynamics into several subsystems. The problem then reduces to the successive stabilization of the individual subsystems, i.e., each step is a submanifold stabilization problem of reduced dimension. In this way, control methods which are only practicable for lower dimensional systems can be applied to the overall complex dynamical system. To ensure that the subsystems can be stabilized independently, the dynamics are transformed by a change of coordinates to a form with block-diagonal inertia metric. For the unactuated part kinetic symmetries can be utilized, whereas for the actuated part null space projectors are employed to decouple the dynamics with respect to the inertia metric. The subsystems are then stabilized by optimal control or PD-like feedback. In the stability analysis semidefinite Lyapunov functions are employed. The procedure is demonstrated for a manipulator on an elastic base and validated in simulation.

Keywords: Hamiltonian dynamics; Robotics; Nonlinear control

1. INTRODUCTION

Underactuated mechanical systems are typically characterized by having fewer control inputs than degrees of freedom (DOF) (see Spong (1994); Olfati-Saber (2001)). Underactuated mechanical systems arise in various kinds of fields, such as robotics, aerospace and naval systems. Prominent examples in robotics are locomotion systems and manipulators with elasticities or free floating base. While fully actuated systems are (exact) feedback linearizable (see, e.g., Isidori (1995)), the problem for underactuated systems is more difficult. The major obstruction stems from the fact that only one part of the mechanical system can be directly accessed by the control input. It is considered that the remaining part of the dynamics is subject to a constraint, which is sometimes referred to as a nonholonomic second-order or acceleration constraint (Olfati-Saber (2001)). The dynamics of the system are typically described by the Lagrange equations of motion

$$M(q)\ddot{q} + C(q,\dot{q})\dot{q} + \frac{\partial V}{\partial q} = B\tau, \tag{1}$$

which are a very popular form of representation used in robotics. The configuration $q \in \mathbb{R}^n$ is a coordinate of the configuration manifold $\mathcal{Q}$. The positive definite inertia matrix $M(q) \in \mathbb{R}^{n\times n}$ is the coordinate expression of the metric g of the mechanical system and $V(q)$ denotes the potential energy. Moreover, the Coriolis matrix $C(q,\dot{q}) \in \mathbb{R}^{n\times n}$ is chosen such that $\dot{M}(q) - 2C(q,\dot{q})$ is skew symmetric. Furthermore, the vector $\tau \in \mathbb{R}^d$ denotes the control input and $B = [0\ I]^\top \in \mathbb{R}^{n\times d}$ is the input matrix.

The remaining paper is structured as follows. In the two subsequent subsections an overview on selected control strategies is given and the contribution of this paper is stated. Section 2 summarizes the preliminaries on stable manifolds and the Hamilton-Jacobi equation from a symplectic point of view. Moreover, the successive reduction procedure is presented in subsection 2.2, which is then applied in section 3 to control a d-link manipulator on a flexible base with a single rotational DOF. Section 3 itself presents the considered model and control goal, the successive control design, stability analysis and a numerical simulation. Finally, the work is concluded in section 4.

1.1 Related Work

The following list of methods makes no claim of completeness and considers approaches which stabilize an equilibrium point. A widely applicable and very popular procedure was proposed in Spong (1994) which is commonly known as partial feedback linearization for underactuated systems. The design process involves finding an output

⋆ This project has received funding from the European Research Council (ERC) under the European Union's Horizon 2020 research and innovation programme (grant agreement No. 819358). The work of the second author is supported, in part, by JSPS KAKENHI Grant Number JP19K04446 and by Nanzan University Pache Research Subsidy I-A-2 for 2021 academic year.

function which is then controlled to be identically zero. To guarantee that the output can be stabilized a common approach is to choose the output such that it has a well defined vector relative degree (see, e.g., Isidori (1995)) of two everywhere. The stability of the overall dynamics is typically analyzed investigating the zero dynamics. In Olfati-Saber (2001), these ideas are further developed and changes of coordinates were proposed to transform the equations of motion into the corresponding normal forms. Depending on the structure of the normal form, different kind of control strategies, for example backstepping methods, are proposed. Another approach which allows to handle underactuation is Immersion and Invariance, which was proposed by Astolfi and Ortega (2003). Here, the input affine control system is stabilized by rendering a manifold asymptotically stable and invariant. On this lower dimensional submanifold the system follows a desired target dynamics $\dot{\xi} = \alpha(\xi)$, which exhibits a globally asymptotically stable equilibrium point ξ^*. In order to realize the stabilization of the manifold by control, the so-called immersion condition must be satisfied. Finding a solution to this set of partial differential equations (PDEs) is in general not trivial and constitutes a key step in the control design. The interconnection and damping assignment passivity based control (IDA-PBC) framework is also applied to underactuated mechanical systems in Ortega et al. (2002). In order to comply with the second order nonholonomic constraint, in the control design the so-called matching conditions have to be satisfied. The matching conditions constitute a PDE for the desired potential energy function as well as the metric tensor of the closed-loop system.

A fundamentally different approach to control underactuated mechanical systems is to design a controller, which is optimal with respect to a certain cost function. For quadratic costs, the optimal feedback control can be derived from a solution of the Hamilton-Jacobi equation (HJE), see for example Lee and Markus (1967). Finding such a solution for the PDE given by the HJE can be challenging. A comprehensive overview of the problem can be found in Guckenheimer and Vladimirsky (2004). The stable manifold method introduced in Sakamoto and van der Schaft (2008) tackles the optimal control problem for input affine control systems from a symplectic perspective and proposes to utilize an approximation of the stable manifold by convergent series. The approach is successfully applied to the pendulum on a cart and the acrobot in Horibe and Sakamoto (2016, 2018). However, especially for very complex and high dimensional underactuated mechanical systems, the numerical computation of the feedback law gets very expensive.

1.2 Contribution

The control design for underactuated mechanical systems typically involves solving a PDE, e.g. the matching or immersion condition as well as the HJE, which for high dimensional systems can be complex. In order to reduce this complexity, the dynamics are split into several subsystems. The control problem then reduces to the successive stabilization of the individual subsystems, i.e. each step is a submanifold stabilization problem of lower dimension. Compared to existing approaches the proposed procedure allows to break down the overall complex problem into multiple nested subproblems that are simpler to address. Additionally, in this way sophisticated control methods, which are often only applicable to lower dimensional systems, can be employed to stabilize the overall complex dynamical system. Another promising application could be the embedding of so-called template models of reduced order, see for example Poulakakis and Grizzle (2009); Kurtz et al. (2019). To ensure that the subsystems can be stabilized independently, the dynamics are transformed by a change of coordinates to a form with block-diagonal inertia metric. For the unactuated part, system properties, as for example kinetic symmetries (Olfati-Saber (2001)), can be used to achieve this. While for the actuated part, null space projectors, which play a key role in hierarchical impedance control (Ott et al. (2015)), can be employed to (actively) decouple the dynamics with respect to the inertia metric. The individual subsystems are then stabilized by nonlinear optimal control or a PD-like feedback.

To demonstrate the feasibility and performance of the proposed method, it is applied to control a manipulator which is mounted on a flexible base. With the increased demand for dexterous, mobile and lightweight robotic systems this problem became relevant in many robotic applications. Scenarios range from space mission, humanoid robots, aircraft cleaning, hazardous remoted applications like in nuclear and chemical plants or industrial cranes (see, e.g. Lew and Moon (2001); George and Book (2003)). Previous works typically require assumptions, such as separation of the base and end-effector motion in time-scale or consider a translationally flexible base only as Beck et al. (2019), or do not provide a proof of stability. In this work a rotationally flexible base is considered which constitutes a pertinent problem for the medical robot MIRO with seven DOFs. Having eight DOFs in total, a direct application of the stable manifold method or for example IDA-PBC is nowadays computationally very demanding as it involves solving a nonlinear PDE.

2. STABLE MANIFOLDS AND REDUCTION

In this section, we briefly review preliminaries and the stable manifold method for designing optimal control in nonlinear systems. Furthermore, the proposed successive reduction procedure is presented in subsection 2.2.

To derive the optimal control law, the dynamical system (1) is reformulated into first order ordinary differential equations (ODEs) in form of a nonlinear affine system

$$\dot{x} = f(x) + g(x)u, \tag{2}$$

where $x = (q, \dot{q}) \in T\mathcal{Q}$. Furthermore, it is assumed that there exists an input transformation $\tau = u^* + u$, such that for the desired configuration q^*, the point $x^* = (q^*, 0)$ is an equilibrium point for $u = 0$. Define the quadratic cost function as

$$J = \frac{1}{2}\int_0^\infty x^\top Q x + u^\top R u \, dt, \tag{3}$$

where $R \in \mathbb{R}^{m\times m}$ and $Q \in \mathbb{R}^{n\times n}$ are positive-definite matrices. The optimal control is given by

$$u = -R^{-1} g(x)^\top p, \tag{4}$$

where p satisfies the well-known Hamilton-Jacobi equation

$$H(x,p) = p^\top f(x) - \frac{1}{2} p^\top g(x) R^{-1} g(x)^\top p + \frac{1}{2} x^\top Q x = 0. \tag{5}$$

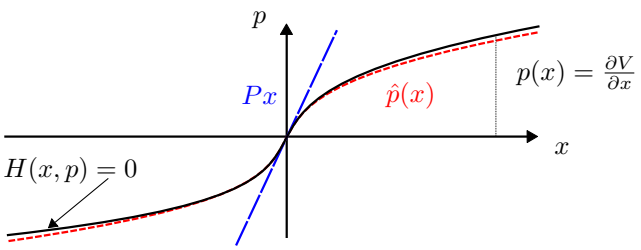

Fig. 1. The stable manifold method approximates $p(x)$ by $\hat{p}(x)$.

Let $\mathcal{M}$ be an m dimensional manifold with coordinates $x^1, \ldots, x^m$. In the following, the HJE is regarded as a first order PDE of the form

$$H(x^1, \ldots, x^m, p^1, \ldots, p^m) = 0, \tag{6}$$

where $p^i = \partial V / \partial x^i$, $i = 1, \ldots, m$ with unknown function $V(x)$ and H is a C^∞ function of $2m$ variables. The cotangent bundle $T^*\mathcal{M}$ with canonical symplectic form $\omega = \sum_j dx^j \wedge dp^j$ is a symplectic manifold. It is assumed that the associated Hamiltonian system

$$\dot{x} = \frac{\partial H}{\partial p}, \quad \dot{p} = -\frac{\partial H}{\partial x} \tag{7}$$

has an equilibrium at $(x, p) = (0, 0)$ and that the linearization of the Hamiltonian system at the equilibrium is hyperbolic, namely, no eigenvalue is on the imaginary axis. The stable manifold $S \subset T^*\mathcal{M}$ of an invariant submanifold $U \subset T^*\mathcal{M}$ is defined as

$$S = \{m \in T^*\mathcal{M} | \lim_{t \to \infty} \Phi^t(m) \in U\}, \tag{8}$$

where $\Phi^t(m)$ denotes the flow of a dynamical system which passes through m at time $t = 0$. It is clear from the definition that the stable manifold itself is an invariant manifold. For more details see for example Wiggins (1994). Let S be the stable manifold of the desired equilibrium in a neighborhood of $(x, p) = (0, 0)$, which is an n-dimensional submanifold. Assume finally that on S, the canonical projection $(x, p) \mapsto x$ is locally surjective. Then, there exists a function $V(x)$ defined in a neighborhood of $x = 0$ such that

$$H(x^1, \ldots, x^n, \partial V/\partial x^1, \ldots, \partial V/\partial x^n) = 0,$$

and S is represented as $\{(x, p) \,|\, p = \partial V/\partial x\}$ in the neighborhood.

2.1 Stable Manifold Method

In the stable manifold method, instead of finding $V(x)$ for (6) directly, one computes S numerically for (7) by using an algorithm that converges to trajectories on S to get

$$\{(x(t), p(t)) \,|\, \text{satisfying (7) and } (x(t), p(t)) \to 0 \text{ as } t \to \infty\}.$$

This data set gives an approximation $\hat{p}(x)$ for $p(x) = \partial V/\partial x$ which is necessary in the feedback law for optimal control, see Fig. 1. Locally at the equilibrium, the optimal control (4) is linearly approximated by the solution P of the algebraic Riccati equation. Therefore, it can be regarded as the extension of the linear quadratic regulator on larger neighborhood. This is how we compute optimal control for regulator problems such as (2)-(3). See van der Schaft (1991, 1992); Sakamoto and van der Schaft (2008); Sakamoto (2013) for more details.

2.2 Successive Reduction

In the following, an overview of the proposed successive reduction approach is given. The described steps are later applied to a manipulator mounted on an elastic base in section 3.

Choice of Unactuated Coordinates (Step 1) Find coordinates for $T\mathcal{Q}$ such that the unactuated velocities are orthogonal to the actuated velocities with respect to metric g. The metric expressed in those coordinates has a block diagonal structure for the unactuated and actuated parts.

Initial Submanifold (Step 2) Verify that the desired configuration q^* is an equilibrium of the unactuated dynamics and, if necessary, perform an input transformation, $\tau = u^* + u$, such that for $u = 0$ the system has an equilibrium point at $(q^*, 0) \in T\mathcal{Q}$. The set $S_0 = \{((q^*, 0), 0)\} \subset T^*T\mathcal{Q}$ is now invariant and S_0 is a symplectic submanifold of $T^*T\mathcal{Q}$. For future use, i is set to one.

Reduction (Step 3) Let S_{i-1} be a stable manifold of a subbundle $B_{i-1} \subset T^*T\mathcal{Q}$, on which solutions of a Hamiltonian system with $H_{i-1}(x_{i-1}, p_{i-1})$, where (x_{i-1}, p_{i-1}) are the coordinates on B_{i-1}, are invariant and exponentially converge to the equilibrium as $t \to \infty$. We find a submanifold S_i of a subbundle B_i with $B_{i-1} \subset B_i$, $S_{i-1} \subset S_i$ such that it is invariant under a Hamiltonian system with $H_i(x_i, p_i)$ and the solutions exponentially converge to S_{i-1}. Writing $x_i = (x_{i-1}, \xi)$, $p_i = (p_{i-1}, \eta)$ in B_i, such S_i is constructed by solving a HJE $H_i(\xi, \eta) = 0$ with $\eta = \partial V_i/\partial \xi$, which can be typically done using a HJE defined by a suitable function H_i as described in subsection 2.1.

Successive Reduction (Step i+2) Repeat Step 3 with increased i until $\dim S_i = 2 \dim T\mathcal{Q}$. In this case, S_i is a Lagrangian submanifold of $T^*T\mathcal{Q}$.

3. BASE VIBRATION CONTROL FOR MANIPULATORS

3.1 Considered Model and Control Goal

In the following, the dynamics of an d-link manipulator [1] attached to an unactuated elastic base with a single rotational DOF are presented. The considered manipulator has d rotational joints and the base elasticity exhibits a nonlinear spring characteristics. The configuration manifold $\mathcal{Q}$ is an $n = d+1$ dimensional torus $\mathbb{T}^n = \mathbb{S}^1 \times \cdots \times \mathbb{S}^1$ with coordinate charts of the form $(\mathcal{U}, q^1, \ldots, q^n)$. Here, q^1 corresponds to the base coordinate. The elastic potential energy of the spring is $V_s(q)$ and the potential energy due to gravity is denoted by $V_g(q)$. In the equations of motion (1), the potential energy is $V(q) = V_s(q) + V_g(q)$. The goal of the control design is to find a control action $\tau \in \mathbb{R}^d$ such that a desired configuration q^* is stabilized. Consequently, the actuators of the manipulator should be employed to steer the robot arm to q^*, while additionally ensuring that the base vibrations are damped. Since the base is unactuated, the desired configuration q^* of the system must coincide with a corresponding natural equilibrium of the base coordinate. For the control design it

[1] The successive stabilization is relevant for $d \geq 2$.

is assumed, that the full state q and $\dot{q}$ are measured or accuratly estimated by an observer.

3.2 Control Design

The derivation of the control law is split into four steps. First the unactuated coordinates are selected. Thereupon, the initial submanifold is determined. Finally, two reduction stages are performed.

Choice of Unactuated Coordinates In order to find coordinates for $T\mathcal{Q}$ such that the unactuated coordinates are orthogonal with respect to metric g to the actuated coordinates, a so-called kinetic symmetry is utilized Olfati-Saber (2001). When the manipulator arm moves freely (no potential forces), the kinetic energy T of the system is independent of the base coordinate q^1. Additionally, the angular momentum l of the system defined along the base joint axis is an integral of motion in this case. When potential forces are added, the angular momentum is not constant anymore but the kinetic symmetry property is conserved as it depends on the inertia tensor only. The new coordinates of $T\mathcal{Q}$ are obtained by replacing the base velocity coordinate by the angular momentum l, induced by the diffeomorphism J_0 defined by

$$\dot{q} = \begin{bmatrix} J_{0,l}(q) & J_{0,a}(q) \end{bmatrix} \begin{bmatrix} l \\ a \end{bmatrix} = J_0(q) \begin{bmatrix} l \\ a \end{bmatrix}, \tag{9}$$

where $a = (q^2, \dots, q^n)$ are the actuated joint velocities and $J_{0,l}(q)$ and $J_{0,a}(q)$ are the corresponding block matrices. Using (9) and its first derivative with respect to time, the velocity dynamics can be expressed in the new coordinates, which yield

$$\begin{bmatrix} \Lambda_l(q)\dot{l} \\ \Lambda_a(q)\dot{a} \end{bmatrix} + \begin{bmatrix} \Gamma_l(q,l,a) \\ \Gamma_a(q,l,a) \end{bmatrix} \begin{bmatrix} l \\ a \end{bmatrix} + J_0(q)^\top \frac{\partial V}{\partial q} = \begin{bmatrix} 0 \\ \tau_0 \end{bmatrix}. \tag{10}$$

The new right hand side is given by $J_0(q)^\top B\tau$, in which the first element is zero and the remaining elements are denoted by τ_0. The metric expressed in the new coordinates is given by $J_0(q)^\top M(q) J_0(q)$. Moreover, the corresponding Coriolis matrix is $J_0(q)^\top C(q,\dot{q}) J_0(q) + J_0(q)^\top M(q) \dot{J}_0(q,\dot{q})$. The special choice of J_0 is compatible with the second order nonholonomic constraint induced by the underactuation of the base, i.e. this implies that the leading element on the right hand side of (10) is zero. The second order dynamics (1) is now expressed in two first order equations in form of (9) and (10). This originates from the fact that the angular momentum is not integrable, i.e., there is no smooth function $h_l : \mathcal{Q} \to \mathbb{R}$ such that $\partial h_l / \partial q \; \dot{q} = l$.

Initial Submanifold The desired equilibrium is given by the desired configuration $q = q^*$ and $l = 0$ as well as $a = 0$. As there is no input available in the first equation of (10), the potential forces affecting the angular momentum dynamics must vanish at the desired configuration and $B\tau_0 = u^* + Bu$ with $u^* = J_0(q)^{-\top} \frac{\partial V}{\partial q}(q^*)$. Therefore, the initial symplectic submanifold in stage 0 is $S_0 = \{((q^*, 0), 0)\} \subset T^*T\mathcal{Q}$.

Reduction Stage 1 The configuration of the manipulator is described by d independent variables $q^2, \dots, q^n$. In order to stabilize the angular momentum dynamics the configuration manifold of the manipulator is decomposed into two regular submanifolds of dimension 1 and $d-1$, which are represented by $h_v : \mathcal{Q} \to \mathbb{R}$ and $h_r : \mathcal{Q} \to \mathbb{R}^{d-1}$ as charts, such that the product of both submanifolds is diffeomorphic to the configuration manifold of the manipulator. As the charts represent the manipulator configuration, they are independent of the base coordinate, i.e., $dh_v(\frac{\partial}{\partial q^1}) = 0$ and $dh_r(\frac{\partial}{\partial q^1}) = 0$. Considering local coordinates, it is assumed that the charts are centered at the desired configuration, i.e., $h_v(q^*) = 0$ and $h_r(q^*) = 0$. Basis for the control design in this stage is that $h_r(q) = 0$ and that the remaining velocity $r = \partial h_r / \partial q \; \dot{q}$ is equal to zero. For the coordinate h_v a control action is designed, which yields a four dimensional stable manifold $S_1 \subset T^*T\mathcal{Q}$ of S_0. Inertial couplings between h_v and h_r complicate the control design. This is due to the fact that a coupling by the inertia matrix tightly interconnects the dynamics of the two subsystems. A non-zero acceleration in one subsystem results in an acceleration in the other subsystem and vice versa. This also holds for the inputs to the individual subsystems, which are mapped by the inverse inertia matrix. Therefore, the null space projector concept is utilized to define another coordinate transformation J_1

$$\begin{bmatrix} l \\ a \end{bmatrix} = \begin{bmatrix} I & 0 & 0 \\ 0 & Z(q)^\top & Q(q)^{\Lambda_a(q)+} \end{bmatrix} \begin{bmatrix} l \\ n \\ r \end{bmatrix} = J_1(q) \begin{bmatrix} l \\ n \\ r \end{bmatrix}, \tag{11}$$

where $Q = \partial h_r / \partial q \; J_{0,a}$ corresponds to the matrix selecting the remaining velocities r out of a and Q^{W+} denotes the W weighted pseudo inverse of Q defined by $W^{-1}Q^\top (QW^{-1}Q^\top)^{-1}$. Furthermore, $Z(q)^\top$ is the null space matrix of $Q(q)$ satisfying $Q(q)Z(q)^\top = 0$ for all $q \in \mathcal{Q}$ and $\partial h_v / \partial q \; J_{0,a} Z^\top$ is the identity. More details on the null space projector can be found in Ott et al. (2015). The corresponding null space projector slightly differs from the joint space decomposition by a normalization factor, which was initially proposed by Park et al. (1999). The zeros in the lower left corner of J_1 are compatible with the second order nonholonomic constraint. The dynamics in the new coordinates are given by

$$\dot{q} = J(q) \begin{bmatrix} l \\ n \\ r \end{bmatrix}, \tag{12}$$

$$\begin{bmatrix} \Lambda_l(q)\dot{l} \\ \Lambda_n(q)\dot{n} \\ \Lambda_r(q)\dot{r} \end{bmatrix} + \begin{bmatrix} \Gamma_l(q,l,n,r) \\ \Gamma_n(q,l,n,r) \\ \Gamma_r(q,l,n,r) \end{bmatrix} \begin{bmatrix} l \\ n \\ r \end{bmatrix} + \begin{bmatrix} \gamma_l(q) \\ \gamma_n(q) \\ \gamma_r(q) \end{bmatrix} = \begin{bmatrix} 0 \\ \tau_n \\ \tau_r \end{bmatrix}, \tag{13}$$

where $J(q) = J_0(q) J_1(q)$. Furthermore, $\gamma(q) = J(q)^\top \frac{\partial V}{\partial q}(q)$ is partitioned into the corresponding sub blocks γ_l, γ_n, and γ_r. As before, the inertia matrix and the inputs transform via the velocity mapping (here $J_1(q)$). A straightforward calculation reveals $\Lambda_n(q) = Z(q)^\top \Lambda_a(q)^{-1} Z(q)$ and $\Lambda_r(q) = (Q(q)\Lambda_a(q)^{-1}Q(q)^\top)^{-1}$. The off-diagonal terms are given by $Z(q)\Lambda_a(q)Q(q)^{\Lambda_a(q)+}$ and its transpose, which are zero due to the property $Q(q)Z(q)^\top = 0$. Therefore, the inertia matrix exhibits the envisioned block diagonal structure. The input splits into $\tau_n = Z(q)\tau_0$ and $\tau_r = \left(Q(q)^{\Lambda_a(q)+}\right)^\top \tau_0$.

Under the assumption that h_r and remaining velocities r are zero, the velocity n is integrable, i.e., $n = \partial h_v / \partial q \; \dot{q}$, and the reduced dynamics is given by

$$\dot{q} = J_0(q) \begin{bmatrix} I & 0 \\ 0 & Z(q)^\top \end{bmatrix} \begin{bmatrix} l \\ n \end{bmatrix}, \tag{14}$$

$$\begin{bmatrix} \Lambda_l(q)\dot{l} \\ \Lambda_n(q)\dot{n} \end{bmatrix} + \begin{bmatrix} \Gamma_l(q,l,n,0) \\ \Gamma_n(q,l,n,0) \end{bmatrix} \begin{bmatrix} l \\ n \\ 0 \end{bmatrix} + \begin{bmatrix} \gamma_l(q) \\ \gamma_n(q) \end{bmatrix} = \begin{bmatrix} 0 \\ \tau_n \end{bmatrix}. \tag{15}$$

As (14) is subject to the constraint $h_r = 0$ the configuration q is determined by q^1 and h_v. Using $x_1 = (q^1, h_v, l, n)$ as coordinates, the equations above are reformulated in form of (2) with corresponding $f_1(x_1)$ and $g_1(x_1)$. The cost is defined using (3) for appropriate R_1 and Q_1. This yields a HJE of the form $H_1(x_1, p_1) = 0$. In order to verify if a stable manifold exists it can be checked, whether the Riccati equation obtained by the linearization of (5) has a stabilizing solution. If this is not the case, then h_v and h_r have to be altered. The stabilizing control law in form of (4) yields

$$u_n = -R_1^{-1} g_1(x_1) p_1(x_1), \tag{16}$$

where $p_1(x_1) = \frac{\partial V_1}{\partial x_1}$ and $V_1(x_1)$ is the solution to the HJE from above. Here, $p_1(x_1)$ is approximated by the stable manifold method in section 2.1. To apply the control to the manipulator the corresponding part of the input transformation defined by u^* is added, which yields

$$\tau_n = u_n^* + u_n, \tag{17}$$

where $u_n^* = \gamma_n(q^*)$ compensates for the potential forces at the equilibrium.

Reduction Stage 2 To stabilize the dynamics related to r independently of the other dynamics, two options for the input u_r are considered in the following.

The first option is

$$\tau_r = \Gamma_r(q,l,n,r) \begin{bmatrix} l \\ n \\ r \end{bmatrix} + \gamma_r(q) - \Lambda_r(q) R_2^{-1} g_2^\top P_2 x_2, \tag{18}$$

where $x_2 = (h_r, r)$ and P_2 is the solution to the Riccati equation for the linear dynamics $\ddot{h}_r = u_r$ with $f_2(x_2) = [r\ 0]^\top$ and $g_2 = [0\ I]^\top$ and cost given by (3) with appropriate matrices R_2 and Q_2. Therefore, locally there exists a stable manifold $S_2 \subseteq T^*T\mathcal{Q}$ of S_1. The closed-loop dynamics on S_2 is given by the flow along the stable manifold of S_1 and solutions starting in S_2 converge to S_1 for $t \to \infty$. The stability of the closed loop will be analyzed in subsection 3.3.

The second option is to cancel the Coriolis couplings and gravity terms and to apply PD-like control. The control input is given by

$$\tau_r = \Gamma_r(q,l,n,r) \begin{bmatrix} l \\ n \\ 0 \end{bmatrix} + \gamma_r(q) - Dr - Kh_r(q). \tag{19}$$

Here, K and D are positive definite matrices. In contrast to (18), the impedance controller preserves the inertia of the subsystem. In practice, this typically yields a lower control effort and a greater robustness against model uncertainties.

The resulting overall control which is applied to the manipulator results in

$$\tau = J(q)^\top \begin{bmatrix} 0 \\ \tau_n \\ \tau_r \end{bmatrix}, \tag{20}$$

where τ_n is chosen as in (17) and τ_r can be selected as either (18) or (19).

3.3 Stability Analysis

The stability of the closed loop is analyzed in a two step approach. First, it is shown that the system converges to the submanifold given by $h_r = 0$ and $r = 0$. In a second step, the dynamics on the submanifold are analyzed and the stability of the overall system is concluded. The proof utilizes semidefinite Lyapunov functions with the following theorem of Iggidr et al. (1996).

Theorem 3.1. (Theorem 2 of Iggidr et al. (1996)). Let χ_0 be an equilibrium point for the dynamical system $\dot{\chi} = f(\chi)$. If there is a neighborhood U of χ_0 and a $\mathcal{C}^1$ function $V : U \to \mathbb{R}$ such that $V(\chi) \geq 0$ and $\dot{V}(\chi) \leq 0$ for all $\chi \in U$ and $V(\chi_0) = 0$ and χ_0 is asymptotically stable on the largest positively invariant set contained in $\{\chi \in U : \dot{V}(\chi) = 0\}$, then χ_0 is an asymptotically stable equilibrium point for $\dot{\chi} = f(\chi)$.

Theorem 3.2. The closed-loop dynamics consisting of (12) and (13) with control input (17) and (18) has an asymptotically stable equilibrium point χ_0. At χ_0, the manipulator has configuration q^* and the base is at rest.

Proof of Theorem 3.2: The coordinates in a neighborhood $U \subset T^*T\mathcal{Q}$ of the desired equilibrium are partitioned as $x_1 = (q^1, h_v, l, n)$ and $x_2 = (h_r, r)$ as well as $p_1 = \frac{\partial V_1}{\partial x_1}$ and $p_2 = \frac{\partial V_2}{\partial x_2}$. The dynamics is given by

$$\dot{x}_1 = \frac{\partial H_1}{\partial p_1}(x_1, p_1) + d_x(x_1, p_1, x_2, p_2), \tag{21}$$

$$\dot{p}_1 = -\frac{\partial H_1}{\partial x_1}(x_1, p_1) + d_p(x_1, p_1, x_2, p_2), \tag{22}$$

$$\dot{x}_2 = \frac{\partial H_2}{\partial p_2}(x_2, p_2), \tag{23}$$

$$\dot{p}_2 = -\frac{\partial H_2}{\partial x_2}(x_2, p_2), \tag{24}$$

where for $i = \{1, 2\}$, H_i is the Hamiltonian function and V_i is the solution of the corresponding HJE presented in the first and second reduction stage. The functions d_x and d_p vanish for x_2 and p_2 equal to zero, i.e., on S_1. The generating function $V_2(x_2) = x_2^\top P_2 x_2$ regarded as function on $T^*T\mathcal{Q}$ is positive semidefinite. Using (23), the derivative of V_2 along the Hamiltonian flow yields

$$\dot{V}_2(x_2) = x_2^\top (P_2 A_2 + A_2^\top P_2 - 2P_2 g_2 R_2^{-1} g_2^\top P_2) x_2, \tag{25}$$

$$= -x_2^\top (Q_2 + P_2 g_2 R_2^{-1} g_2^\top P_2) x_2 \leq 0, \tag{26}$$

where $A_2 = \partial f_2 / \partial x_2$ and the latter equations follows from P_2 being a solution to the algebraic Riccati equation. In order to apply Theorem 3.1, it remains to show that χ_0 is asymptotically stable on the largest positively invariant set contained in the preimage of $\{0\}$ under $\dot{V}_2$. Within the preimage one has $x_2 = 0$ and consequently $p_2 = 0$, therefore one concludes that the system state is contained in S_1 if U is chosen sufficiently small. On S_1, the dynamics is given by (21)-(22) with d_x and d_p being zero. The proof is concluded by realizing that x_1 and p_1 converge to zero on S_1, i.e., χ_0 is asymptotically stable.

Theorem 3.3. The closed-loop dynamics consisting of (12) and (13) with control input (17) and (19) has an asymptot-

ically stable equilibrium point χ_0. At χ_0, the manipulator has configuration q^* and the base is at rest.

Proof of Theorem 3.3: Inserting (19) into (13) leads to

$$\Lambda_r(q)\dot{r} + (\Gamma_{r,r}(q,l,n,r) + D)r + Kh_r(q) = 0, \quad (27)$$

where $\Gamma_{r,r}$ is the corresponding subblock of Γ_r related to r. Let $V : T\mathcal{Q} \to \mathbb{R}$ be the positive semidefinite function

$$V(q,\dot{q}) = \frac{1}{2} r^\top \Lambda_r(q) r + \frac{1}{2} h_r(q)^\top K h_r(q) \geq 0, \quad (28)$$

The time derivative of V, i.e., the Lie derivative along the closed-loop flow, yields

$$\dot{V}(q,\dot{q}) = r^\top(-\Gamma_{r,r}(q,l,n,r) - D + \frac{1}{2}\dot{\Lambda}_r(q,\dot{q}))r \quad (29)$$

$$= -r^\top D r \leq 0. \quad (30)$$

The second equality follows from $\dot{\Lambda}_r(q,\dot{q}) - 2\Gamma_{r,r}(q,l,n,r)$ being skew symmetric, which is commonly referred to as the passivity property. Moreover, $V(\chi_d) = 0$. As before, Theorem 3.1 is applied by showing asymptotic stability of χ_d on the largest positively invariant set contained in the preimage of $\{0\}$ under $\dot{V}$. Within the preimage one has $r = 0$. Inserting this into (27) yields $Kh_r(q) = 0$, i.e., $h_r = 0$ as $K > 0$. By choosing U sufficiently small, one can conclude that the system state is contained in S_1. On S_1 the dynamics is given by $\dot{x}_1 = \frac{\partial H_1}{\partial p_1}(x_1, \frac{\partial V_1}{\partial x_1}(x_1))$, i.e., χ_0 is asymptotically stable. This concludes the proof.

3.4 Simulation

In the following, the procedure is applied to the seven DOF manipulator MIRO [2] on a single DOF rotationally flexible base, see Fig. 2. The configuration of the base is described as q^1 and the manipulator DOF correspond to $q^2, \ldots, q^8$. The elastic potential of the nonlinear elasticity is given by

$$V_s(q) = \frac{1}{2}K_1(q^1)^2 + \frac{1}{2}K_2(q^1)^4, \quad (31)$$

where $K_1 = 100^{\mathrm{Nm}/\mathrm{rad}}$ and $K_2 = 1000^{\mathrm{Nm}/\mathrm{rad}^3}$ are the stiffness coefficients. The desired configuration q^* corresponds to an equilibrium of the base elasticity for the robot configuration. In the reduction stage 1, the manipulator configuration manifold is decomposed into two submanifolds characterized by $h_v = q^3$ and $h_r = (q^2, q^4, \ldots, q^8)$. By this choice the reduced dynamics for $h_r = 0$ is given by a two DOF mechanical system. The reduced dynamics can be regarded as a single DOF manipulator mounted on an elastic base with one rotational DOF, i.e., correspond to the mechanical system depicted in Fig. 2. Here, the actuated manipulator joint is given by q^3 and the unactuated base is described by coordinate q^1. In the base joint the elasticity acts with potential energy $V_s(q^1)$. Intuitively speaking, the control action given by u_r constrains the manipulator to the reduced system depicted in Fig.2. A numerical simulation is performed to demonstrate the effectiveness of the proposed controller. The remaining dynamics was stabilized by (18). The control parameters are chosen as $Q_1 = \mathrm{diag}(100I_2, 0.1I_2)$, $R_1 = 0.05$, $Q_2 = \mathrm{diag}(100I_6, I_6)$ and, $R_2 = 1e^{-5}I_6$. Here, diag denotes the block diagonal matrix created by aligning its arguments on the diagonal and I_j is the identity matrix of dimension j. As is it can seen in Fig. 3, the error for the fully actuated remaining dynamics (solid lines) is converging uniformly to zero,

[2] Please see Hagn et al. (2008) for more details.

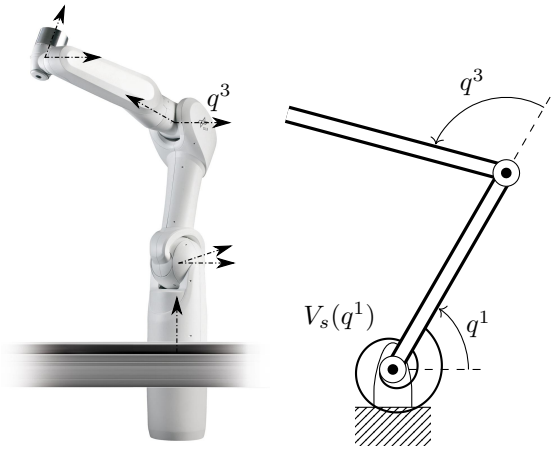

Fig. 2. The MIRO arm (left) and the reduced system given by a single DOF manipulator on elastic base (right).

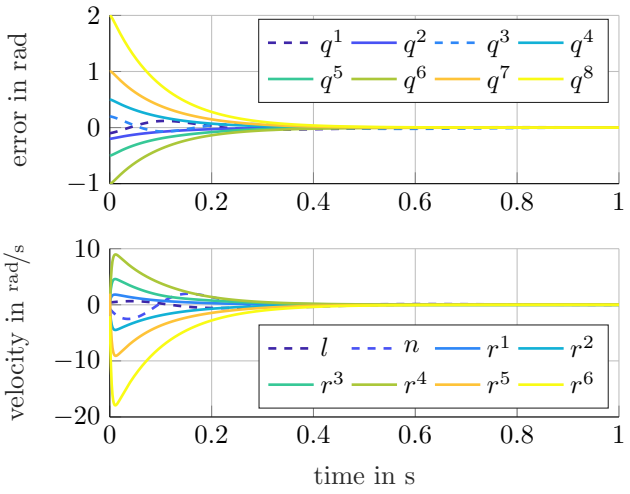

Fig. 3. Simulation of a MIRO manipulator on elastic base.

while for the underactuated reduced system the stable manifold has a more complex geometry (dashed lines).

4. CONCLUDING REMARKS

In this work, a procedure to decompose underactuated mechanical systems was presented. The decomposition can be employed to reduce the overall high dimensional and complex dynamics into multiple subsystems, which are decoupled on the acceleration level. In each stage, the control design is based on the condition that all dynamics on superordinate stages are already converged. Therefore, the dynamical system evolves along the respective subbundle. On the latter, there exists a stable manifold of the subordinate subbundle such that the overall dynamical system is successively stabilized.

Future work may consider different choices of subbundles which would enable to influence the transient behaviour. In the control design of the flexible base manipulator for example, a different choice of the reduced dynamics could reduce the required joint torques or achieve a certain desired end-effector response. Additionally, the presented procedure should be extended to a more global approach allowing for multiple charts. Besides a consistent transition between overlapping charts, the control design should

also take topological obstructions into account. A more global approach would also require modifications in the stability analysis as well as the computation of the stable manifold approximation, as both are currently only locally applicable. Finally, the approach could be employed to embed template models in underactuated systems, which were already successfully applied in bipedal locomotion.

REFERENCES

Astolfi, A. and Ortega, R. (2003). Immersion and invariance: A new tool for stabilization and adaptive control of nonlinear systems. *IEEE Transactions on Automatic Control*, 48(4), 590–606.

Beck, F., Garofalo, G., and Ott, C. (2019). Vibration control for manipulators on a translationally flexible base. In *International Conference on Robotics and Automation*, 4451–4457. IEEE.

George, L.E. and Book, W.J. (2003). Inertial vibration damping control of a flexible base manipulator. *IEEE/ASME Transactions on Mechatronics*, 8(2), 268–271.

Guckenheimer, J. and Vladimirsky, A. (2004). A Fast Method for Approximating Invariant Manifolds. *SIAM Journal on Applied Dynamical Systems*, 3(3), 232–260.

Hagn, U., Nickl, M., Jörg, S., Passig, G., Bahls, T., Nothhelfer, A., Hacker, F., Le-Tien, L., Albu-Schäffer, A., Konietschke, R., Grebenstein, M., Warpup, R., Haslinger, R., Frommberger, M., and Hirzinger, G. (2008). The DLR MIRO: A versatile lightweight robot for surgical applications. *Industrial Robot: An International Journal*, 35(4), 324–336.

Horibe, T. and Sakamoto, N. (2016). Swing up and stabilization of the acrobot via nonlinear optimal control based on stable manifold method. *IFAC-PapersOnLine*, 49(18), 374–379.

Horibe, T. and Sakamoto, N. (2018). Optimal swing up and stabilization control for inverted pendulum via stable manifold method. *IEEE Transactions on Control Systems Technology*, 26(2), 708–715.

Iggidr, A., Kalitine, B., and Outbib, R. (1996). Semidefinite lyapunov functions stability and stabilization. *Mathematics of Control, Signals and Systems*, 9(2), 95–106.

Isidori, A. (1995). *Nonlinear control systems*. Springer-Verlag, Berlin.

Kurtz, V., Silva, R.R.d., Wensing, P.M., and Lin, H. (2019). Formal Connections between Template and Anchor Models via Approximate Simulation. In *IEEE-RAS 19th International Conference on Humanoid Robots (Humanoids)*, 64–71.

Lee, E.B. and Markus, L. (1967). *Foundations of Optimal Control Theory*. Wiley.

Lew, J.Y. and Moon, S.M. (2001). A simple active damping control for compliant base manipulators. *IEEE/ASME Transactions on Mechatronics*, 6(3), 305–310.

Olfati-Saber, R. (2001). *Nonlinear control of underactuated mechanical systems with application to robotics and aerospace vehicles*. Ph.D. thesis.

Ortega, R., Spong, M.W., Gomez-Estern, F., and Blankenstein, G. (2002). Stabilization of a class of underactuated mechanical systems via interconnection and damping assignment. *IEEE Transactions on Automatic Control*, 47(8), 1218–1233.

Ott, C., Dietrich, A., and Albu-Schäffer, A. (2015). Prioritized multi-task compliance control of redundant manipulators. *Automatica*, 53, 416–423.

Park, J., Chung, W., and Youm, Y. (1999). On dynamical decoupling of kinematically redundant manipulators. In *Proceedings IEEE/RSJ International Conference on Intelligent Robots and Systems*, volume 3, 1495–1500.

Poulakakis, I. and Grizzle, J.W. (2009). The Spring Loaded Inverted Pendulum as the Hybrid Zero Dynamics of an Asymmetric Hopper. *IEEE Transactions on Automatic Control*, 54(8), 1779–1793.

Sakamoto, N. (2013). Case studies on the application of the stable manifold approach for nonlinear optimal control design. *Automatica*, 49(2), 568–576.

Sakamoto, N. and van der Schaft, A.J. (2008). Analytical approximation methods for the stabilizing solution of the Hamilton-Jacobi equation. *IEEE Transactions on Automatic Control*, 53(10), 2335–2350.

Spong, M.W. (1994). Partial feedback linearization of underactuated mechanical systems. In *Proceedings of IEEE/RSJ International Conference on Intelligent Robots and Systems*, volume 1, 314–321. IEEE.

van der Schaft, A.J. (1991). On a state space approach to nonlinear H_∞ control. 16(1), 1–18.

van der Schaft, A.J. (1992). L_2-gain analysis of nonlinear systems and nonlinear state feedback H_∞ control. 37(6), 770–784.

Wiggins, S. (1994). *Normally Hyperbolic Invariant Manifolds in Dynamical Systems*. Applied Mathematical Sciences. Springer-Verlag, New York.